ELSEVIER

Biophysical Chemistry 72 (1998) 111–121

Biophysical Chemistry

A model of mitochondrial Ca^{2+}-induced Ca^{2+} release simulating the Ca^{2+} oscillations and spikes generated by mitochondria

Vitalii A. Selivanov[a,b], François Ichas[a], Ekhson L. Holmuhamedov[c], Laurence S. Jouaville[a], Yuri V. Evtodienko[d], Jean-Pierre Mazat[a,*]

[a]*GESBI, D(BM)$_2$, Université Victor Segalen, F-33076 Bordeaux cedex, France*
[b]*Belozersky Institute, Moscow State University, Moscow, 119899, Russia*
[c]*NASA Ames Research Center, Moffett Field, CA 94035–1000, USA*
[d]*ITEB, Russian Academy of Sciences, Pushchino, 142292, Russia*

Revision received 19 January 1998; accepted 13 February 1998

Abstract

Recent evidence underlines a key role of mitochondrial Ca^{2+} fluxes in cell Ca^{2+} signalling. We present here a kinetic model simulating the Ca^{2+} fluxes generated by mitochondria during mitochondrial Ca^{2+}-induced Ca^{2+} release (mCICR) resulting from the operation of the permeability transition pore (PTP). Our model connects the Ca^{2+} fluxes through the ruthenium red-sensitive Ca^{2+} uniporter, the respiration-dependent and passive H^+ fluxes, the rate of oxygen consumption, the movements of weak acids across the mitochondrial membrane, the electrical transmembrane potential ($\Delta\Psi$), and operation of the PTP. We find that two factors are crucial to account for the various mCICR profiles that can be observed experimentally: (i) the dependence of PTP opening and closure on matrix pH (pH_i), and (ii) the relative inhibition of the respiratory rate consecutive to PTP opening. The resulting model can simulate irreversible Ca^{2+} efflux from mitochondria, as well as the genesis of damped or sustained Ca^{2+} oscillations, and of single Ca^{2+} spikes. The model also simulates the main features of mCICR, i.e. the threshold-dependence of mCICR triggering, and the all-or-nothing nature of mCICR operation. Our model should appear useful to further mathematically address the consequences of mCICR on the spatiotemporal organisation of Ca^{2+} signals, as a 'plug-in' module for the existing models of cell Ca^{2+} signalling. © 1998 Elsevier Science B.V. All rights reserved

Keywords: Mitochondria; Cell calcium signalling; Model of calcium oscillations and spikes; Mitochondrial calcium-induced-calcium-release; Permeability transition pore

1. Introduction

In many cells, the information provided by external stimuli, either electrical, hormonal, photochemical, or mechanical, is conveyed within the cytoplasm by Ca^{2+} signals that take the form of Ca^{2+} oscillations and waves [1]. The information is encoded by the spatio-temporal organisation of these signals, and the latter determines the subsequent cellular responses [2]. The main mechanism underlying the organisation of the cytosolic Ca^{2+} signals is autocatalytic and termed 'Ca^{2+}-induced Ca^{2+} release' (CICR) [1,3,4]. The

* Corresponding author. Fax: +33 05 57571612; e-mail jpm@u-bordeaux2.fr

0301-4622/98/$19.00 © 1998 Elsevier Science B.V. All rights reserved
PII S0301-4622(98)00127-6

CICR machinery is usually identified with the sole endoplasmic reticulum (ER), and thought to rely principally on Ca^{2+}-activable Ca^{2+} channels of the ER membrane, i.e. the inositol 1,4,5-trisphosphate (IP_3) and ryanodine receptors (IP_3R and RyR, repectively) [1,3,4]. However, when Ca^{2+} is released from the ER at locally high concentration, the neighbouring mitochondria take up some of it as shown by aequorin addressed to mitochondria [5]. This results in a modification of the spatiotemporal organisation of the Ca^{2+} signals [6–8]. Two types of mechanisms can be proposed to account for such mitochondrial effect: (i) a regulation of IP_3R activity by local mitochondrial Ca^{2+} buffering, modulating the ER CICR [6], and (ii) a Ca^{2+}-stimulated operation of mitochondrial Ca^{2+} efflux pathways contributing to the cytosolic Ca^{2+} raise [9,11]. Regarding this last interpretation, one pathway of mitochondrial Ca^{2+} efflux is of particular interest, since it also obeys autocatalytic rules. This pathway, whose operation we termed mCICR [9,10], depends on the transient opening of the PTP by mitochondrial Ca^{2+} uptake, and generates Ca^{2+} spikes [9,10] and oscillations [12,13] in vitro. It should be noticed that in all these experimental observations, the external calcium concentration necessary to trigger oscillations or a spike on isolated mitochondria or mitochondria inside permeabilised cells are rather high, between 60 and 120 μM and that, in these conditions, mitochondria are able to accumulate a large amount of the added calcium. Damped oscillations are induced by 100 μM external calcium on permeabilised Ehrlich ascites tumour cells [12]; the sensitivity of these oscillations to cyclosporin A indicates the participation of PTP in this process. Sustained oscillations are observed with digitonin-treated *Tetrahymena pyriformis* in low Po_2 conditions, i.e. at low respiratory rate [13]. In living cells, mCICR is triggered by IP_3-dependent Ca^{2+} release from the ER, resulting in the amplification of the cytosolic Ca^{2+} signals [9,10], indicating that mitochondria inside cells are either more sensitive to calcium or that high local calcium concentrations can be sensed by mitochondria in the vicinity of ER as demonstrated in [5], or both.

We present here a theoretical analysis of mCICR providing direct information on the mitochondrial determinants of mCICR. We based our mathematical model on the following observations: (i) extramitochondrial Ca^{2+} is taken-up electrophoretically by mitochondria through the ruthenium red-sensitive Ca^{2+} uniporter [14]; (ii) mitochondrial Ca^{2+} uptake causes a transitory drop in $\Delta\Psi$ that results in respiration activation [14]; (iii) activation of respiration, which corresponds to an increased H^+ extrusion, results in the alcalinization of the mitochondrial matrix [14]; (iv) matrix alcalinization activates the PTP [15], and thus triggers various ion fluxes – among those, Ca^{2+} efflux – according to their electrochemical potential; (v) PTP activation also causes a relative respiration inhibition [12] that contributes to matrix acidification; (vi) matrix acidification inactivates the PTP [15].

The resulting model, although it is a very simplified theoretical model, simulates all the known modes and features of mCICR and should thus appear useful to perform mathematical studies of the mitochondrial contribution to cell Ca^{2+} signals as a 'plug-in' module for the already existing models of Ca^{2+} signalling [16–19].

2. The model

The model consists of a system of differential equations describing the following variables: outside Ca^{2+} concentration (Ca), $\Delta\Psi$ ($\Delta\Psi = \Psi_{out} - \Psi_{in}$), inside H^+ concentration (H), the amount of opened PTP channels responsible for unselective mitochondrial membrane permeability (T^{op}), matrix concentration of a respiratory chain activator (A).

The model accounts for the following fluxes across the inner mitochondrial membrane: J_{ca}, Ca^{2+} flux through the ruthenium red-sensitive mitochondrial Ca^{2+} uniporter; J_{an}, anions flux; J_{AH}, flux of the protonated acids; J_H, H^+ leak; J_r, H^+ transport connected with respiration; V_A, rate of production of a respiration activator within the matrix; J_A, efflux of this activator.

We have not included in the model the calcium transport through the activity of the $2Na^+/Ca^{2+}$ nor through the $Ca^{2+}2H^+$ exchangers, because experimentally, spikes have been shown to be generated independently of these exchangers (no Na^+ in the medium) [9,10]. However, it should be noticed that experimental calcium oscillations have been observed in mitochondria in the presence of 100 mM Na [12] which

could indicate a role played by the $2Na^+/Ca^{2+}$ exchanger. Thus our model will appear as a minimal model able to generate calcium oscillations and spikes in mitochondria; for the same reason the ATPase activity is not included.

We use the Goldman equation to describe the various ion fluxes through the inner mitochondrial membrane:

$$J = J^{out} - J^{in} = P\Delta\Psi \frac{C_{in}\exp\left(-zF\frac{\Delta\Psi}{RT}\right) - C_{out}}{1-\exp\left(-zF\frac{\Delta\Psi}{RT}\right)} \quad (1)$$

where J^{in} denotes the ion flux from outside to inside, and J^{out} the opposite flux of the same ion. C_{in} and C_{out} are the ion concentrations inside and outside. $P = p(RT/zF)$, where p is the permeability coefficient of the considered ion, z its charge, F is Faraday's number, R is the gas constant, and T the absolute temperature. In the following text we will use the term 'permeability coefficient' to qualify P.

2.1. Ca^{2+} fluxes through the Ca^{2+} uniporter

The $\Delta\Psi$ dependence of the Ca^{2+} fluxes through the uniporter fits a form consistent with the Goldman constant field equation [20] and therefore can be described by Eq. (1). However, the Ca^{2+} fluxes mediated by the uniporter are not only dependent on transmembrane potential $\Delta\Psi$, but also on the external Ca^{2+} concentration. This is the reason why we included in the Goldman equation the term $(Ca - C_0)$ instead of Ca only, where Ca represents extramitochondrial Ca^{2+} concentration and $C_0 = 0.5$ μM, which is the basal Ca^{2+} concentration above which the uniporter insures a net influx of Ca^{2+} [20,22].

$$J_{Ca} = P_{Ca}\Delta\Psi \frac{Ca_{in}\exp\left(-2F\frac{\Delta\Psi}{RT}\right) - (Ca - C_0)}{1-\exp\left(-2F\frac{\Delta\Psi}{RT}\right)} \quad (2)$$

mCICR is triggered in vitro by extramitochondrial Ca^{2+} concentrations in the range of 60–100 μM. In these conditions, the intra-mitochondrial Ca^{2+} exchangeable with outside Ca^{2+}, determined by null-point titration experiments, is in the same order of magnitude than the outside one [21]. Moreover, because of the high intra-mitochondrial Ca^{2+} buffering power [14], we consider the internal Ca^{2+} concentration as a constant equal to 100 μM (Ca_{in} = 100 μM). It should be noted that the actual free calcium concentration is much lower and can be slightly variable.

P_{Ca} can be determined from the measured value of the maximal Ca^{2+} flux through the uniporter. The maximal value of 1000 nmol min^{-1} mg^{-1} [14,23] can be reproduced by Eq. (2) at $\Delta\Psi$ = 150 mV by taking P_{Ca} = 0.1 min^{-1} mV^{-1} mg $protein^{-1}$. However, the experimental value for the maximal rate of Ca^{2+} uptake is obtained at a lower $\Delta\Psi$, because it is measured in the presence of high outside Ca^{2+} concentration which collapses $\Delta\Psi$. Thus, the highest reported values of V_{max} for the Ca^{2+} uniporter rather reflect the maximal rate of respiration than the maximal rate of Ca^{2+} entry. Thus the real maximal Ca^{2+}-transporting capacity of uniporter can be considered as being higher [14]. For this reason, we set in the model P_{Ca} = 1 min^{-1} mV^{-1} mg $protein^{-1}$.

2.2. Opening and closure of the PTP

Regulation of the PTP is one of the key elements of our model. Three main factors have been shown to induce PTP opening: (i) increase in inside Ca^{2+} concentration; (ii) decrease in $\Delta\Psi$; and (iii) increase in pH_i [15]. Conversely, the opposite changes of the same parameters promote PTP closure. mCICR can be induced by Sr^{2+}, which is not a direct agonist of PTP [22]. Thus, we make the two following assumptions: (i) Ca^{2+} itself is not the trigger for PTP opening during mCICR; and (ii) the amount of Ca^{2+} permanently present inside mitochondria is sufficient to promote PTP opening by pH_i or $\Delta\Psi$. Thus, according to our hypotheses, PTP activation during mCICR is indirectly triggered by Ca^{2+} uptake, but not by Ca^{2+} per se. Since Ca^{2+} uptake decreases $\Delta\Psi$ and raises pH_i, these two factors are still candidate triggers of PTP opening during mCICR. However, the experiments show that during mCICR, PTP opening does not coincide with the minimum $\Delta\Psi$ encountered during the mCICR cycle, and that PTP closure occurs when $\Delta\Psi$ reaches its lowest value [9,10]. Thus, we suppose in our model that $\Delta\Psi$ is not the trigger for PTP opening during mCICR. Regarding the role of pH_i, the max-

imum probability of PTP opening is observed at pH_i above 7.3, while the PTP remains closed at pH_i below 7.0 [15]. During mCICR, we observed experimentally that pH_i is maximal at the time of PTP opening, and minimal at the time of PTP closure [10]. Thus, we consider in our model that pH_i is the only key PTP regulator during mCICR. This assumption will appear below sufficient to account for the various mCICR profiles experimentally observed.

We thus utilise a function f which expresses the effect of pH_i on PTP opening: $f = 1$ if $pH > 7.5$, $f = 0$ if $pH < 7.0$ and f linearly increases from 0 to 1 when pH_i increases from 7.0 to 7.5. With this function, the rate of PTP opening (V_T^{op}) is proportional to the amount of closed channels ($1 - T^{op}$), and to the value of the function f. Conversely, the rate of PTP closure (V_T^{cl}) is proportional to the value of ($1 - f$) and to the amount of opened channels (T^{op}).

Thus, the rates are expressed by the equations:

$$V_T^{op} = k_T^{op} f (1 - T^{op}) \quad (3)$$

$$V_T^{cl} = k_T^{cl} (1 - f) T^{op} \quad (4)$$

The rate constants and are supposed to be equal to 1 min^{-1}.

2.3. Electrogenic ion fluxes through the PTP

The H^+ fluxes through the PTP are described using the general Eq. (1), taking also into account the PTP opening status (T^{op}):

$$J_H = P_H T^{op} \Delta\Psi \frac{H \exp\left(-F\frac{\Delta\Psi}{RT}\right) - H_{out}}{1 - \exp\left(-F\frac{\Delta\Psi}{RT}\right)} \quad (5)$$

In experimental mCICR, outside H^+ concentration (H_{out}) is kept constant by pH buffers [9,12], thus we keep it constant in our model: $H_{out} = 0.1$ μM (pH = 7.0). Inside H^+ concentration (H) is variable. The value of P_H, the coefficient of permeability of the mitochondrial membrane for protons is unknown, but it can be assumed that the H^+ fluxes during maximal PTP opening are of the same order as the Ca^{2+} fluxes. Thus, P_H can easily be estimated. Initial Ca^{2+} concentration pulse is set in our simulation to 30 μM, which is 300 times greater than outside H^+ concentration. Thus, with $P_H = 300$ min^{-1} mV^{-1} mg $protein^{-1}$, the two fluxes are of the same order.

Anion fluxes can be described with the same general Eq. (1), but the following considerations simplify their mathematical description:

Taking into consideration the equilibrium equation for acid dissociation:

$$AH \leftrightarrow [A^-] + [H^+],\ K = \frac{[A^-][H^+]}{[AH]}$$

and the conservation equation:

$[A^-] + [AH] = An$, where An is the total acid concentration, we get the following expression for $[A^-]$:

$$[A^-] = \frac{KAn}{K + [H^+]}$$

At $pH > 7$, $K >> [H^+]$, and thus, we can consider that anion concentration is equal to the total concentration of all acids and their soluble salts, $[A^-] = An$.

Total acid concentration (An), is usually high compared to its changes during mCICR. This is due to the fact that anion variations outside mitochondria are damped by dilution (outside volume = 1000 times matrix volume), and changes in matrix anion concentrations are compensated by osmotic regulation.

Therefore, we will consider anion concentration, inside as well as outside, as a constant An = 10 mM. In these conditions, Eq. (1) for anions simplifies as:

$$J_{An} = -P_{An} T^{op} \Delta\Psi An \quad (6)$$

Concerning P_{An}, the same reasoning as above leads to: $P_{An} = 0.001$ min^{-1} mV^{-1} mg $protein^{-1}$.

Regarding Ca^{2+}, we do not take into account the specific efflux of Ca^{2+} through the PTP because when $\Delta\Psi$ collapses, the efflux of Ca^{2+} through the uniporterer is only limited by proton influx and anion efflux through the PTP. We have experimentally shown that the dissipation of $\Delta\Psi$ leads to Ca^{2+} efflux equally well through the uniporter or through the PTP, because it is not blocked by ruthenium-red or cyclosporin A added separately, but only by the presence of both [22]. For the sake of simplicity, we have only considered in the model the Ca^{2+} efflux through the uniporter. Thus Eq. (2) is sufficient to account for all Ca^{2+} movements through the mitochondrial mem-

brane, independently of the Ca^{2+}-conductive pathway provided by the PTP.

2.4. H^+ ejection by the respiratory chain

The respiration rate, and the corresponding H^+ efflux rate, is constant and maximal if the value of electrochemical transmembrane potential, expressed in electrical units, ($\Delta\mu_{H+} = \Delta\Psi + (RT/F)\Delta pH$; $\Delta pH = pH_i - pH_{out}$) does not exceed 160 mV. The maximal rate (J_{max}) is approximately equal to 1000 nmol $H^+ \times min^{-1} \times mg\ protein^{-1}$. If $\Delta\mu_H + > 160$ mV, we consider that the flux of protons linearly decreases together with the increase of $\Delta\mu_H^+$, and that the flux falls to zero when $\Delta\mu_H^+$ reaches 200 mV.

Thus,

$$\text{If } \Delta\mu_{H^+} > 160\text{mv},\ J'_r = J_{max}\left(1 - \frac{(\Delta\mu_{H^+} - 160)}{40}\right),$$

$$\text{otherwise } J'_r = J_{max} \quad (7)$$

It was shown that the respiration rate undergoes a relative inhibition consecutive to PTP opening, while $\Delta\Psi$ is decreased [12]. The factor, which induces this inhibition is still unknown. We thus suppose here the existence of an activator of respiration, such that the respiration rate is proportional to its intra-mitochondrial concentration:

$$J_r = J'_r A \quad (8)$$

where J'_r is described by Eq. (7), and A is the amount of activator inside the mitochondrial matrix. We do not speculate here on the very nature of the activator, and use it as a phenomenological variable.

We further assume that the relative inhibition of respiration during PTP opening is due to the efflux of activator through the opened PTP. The efflux of activator (J_A) is proportional to its relative amount inside mitochondria, and to the PTP opening state:

$$J_A = P_A[T^{op}][A] \quad (9)$$

where the permeability coefficient P_A is set to 1 min^{-1}.

The production of activator (V_A) is supposed to be dependent on the relative amount of activator inside mitochondria (between 0 and 1). The production is stopped when the activator concentration reaches the relative maximal level of 1 and it linearly increases when the concentration decreases:

$$V_A = k_A(1 - A) \quad (10)$$

where k_A is a constant set to 1 min^{-1}.

To represent respiration in terms of O_2 consumption, we fixed a finite initial oxygen pool of 500 nmol O_2 mg $protein^{-1}$, and assumed a rate of consumption equal to $-J_r/4$.

2.5. $e - \Delta\Psi$

$\Delta\Psi$ changes in response to the described electrogenic ion fluxes correspond to:

$$\frac{d(\Delta\Psi)}{dt} = \frac{F}{C}(J_r + 2J_{Ca} + J_{An} + J_H) \quad (11)$$

where F = 10^5 q/mol = 10^{-4}q/nmol (Faraday number) and C is the electric capacity of the membrane.

The measured specific capacity of biomembranes approaches 1 mF/cm^2 [24] The mitochondrial surface is function of the osmotic pressure, and varies from 1 m^2/g of protein to 30 m^2/g of protein [25]. Experimentally, mCICR operation is favoured by hypo-osmotic conditions [9], due to the sensitisation of the PTP to Ca^{2+} [26]. We thus set here the value of S to 20 m^2/g = 200 cm^2/mg. Therefore C = 200 mF/mg of protein = 2×10^{-4} F/mg of protein. So, $F/C = 0.5\ V$ $nmol^{-1}$ mg protein = 500 mV $nmol^{-1}$ mg protein.

2.6. Electroneutral fluxes of weak acids

During mCICR, the fluxes of weak organic acids, i.e. principally succinate under the reference in vitro conditions [9,12], allow the recovery of pH_i after H^+ respiratory efflux, due to the dissociation of the transported acids inside the matrix. In the particular case of succinate, the latter is transported trough the mitochondrial membrane by a dicarboxylate translocator, in exchange for malate. Using the same translocator, malate goes back into the matrix in exchange for phosphate. Finally the operation of the phosphate transporter exchanges external phosphate for matrix OH^-. In the reference experimental conditions it appears that succinate transport is never a limiting step. Thus, we simplify here the mathematical description of the weak acid fluxes by assuming that succinate is membrane-permeant under its protonated form.

The electroneutral fluxes of permeant weak acids proceed according to the scheme:

$$H_i^+ + A_i^- \overset{1}{\leftrightarrow} HA_i \overset{2}{\leftrightarrow} HA_o \overset{3}{\leftrightarrow} A_o^- + H_o^+ \quad (12)$$

Steps 1 and 3 correspond to the reversible dissociation of the acids, inside (i) and outside (o) mitochondria, step 2 corresponds to the diffusion through the membrane. The rate of diffusion (J) is proportional to the protonated acid (HA) concentrations inside and outside:

$J = k[AH]$, or taking into account equilibrium steps 1 and 3, $J = k_1[A^-][H^+]$, where $k_1 = k/K$.

But since $[A^-] = An$, as shown before, $J = k_{AH}[H^+]$, where $k_{AH} = k_1 An$.

Thus, if inside and outside anion concentrations are equal, as well as the constants of diffusion through the membrane in both directions, the equation giving the net flux of AH is:

$$J_{AH} = J^{out} - J^{in} = k_{AH}(H - H_{out}) \quad (13)$$

where we set k_{AH} to 100 min^{-1} mg $protein^{-1}$, and H_{out} to 0.1 μM (pH = 7).

Other fluxes such as Ca^{2+}/H^+, Ca^{2+}/Na^+, or Na^+/H^+ exchanges, are not taken into account in the model, because they are exceedingly slow in comparison with the fluxes encountered during mCICR (for instance, the rate of Na^+/H^+ exchange is only 0.5 nmol min^{-1}mg $protein^{-1}$ [14]).

2.7. Differential equations of the model

The following system of differential equations describes the behaviour of the variables:

$$\begin{aligned}
\frac{d(Ca)}{dt} &= J_{Ca}/v_{out} \\
\frac{d(\Delta\Psi)}{dt} &= \frac{F}{C}(J_r + 2J_{Ca} + J_{AN} + J_H) \\
\frac{d(H)}{dt} &= (-J_H - J_{AH} - J_r)/B/v_{in} \\
\frac{d(T^{op})}{dt} &= V_T^{op} - V_T^{cl} \\
\frac{d(A)}{dt} &= V_A - J_A
\end{aligned} \quad (14)$$

The ion fluxes are also dependent on the amount of mitochondria undergoing mCICR. On the basis of experimental conditions [9,12] we set it to 1 mg of proteins. The total outside volume V_{out} is set to 1 ml, and the matrix volume V_{in} to 2 μl. The H^+ buffering capacity of the mitochondrial matrix, B, can be estimated by the following consideration: the uptake of Ca^{2+}, at an outside concentration of 20–50 μM, leads to an equivalent efflux of H^+, which corresponds to a matrix H^+ concentration decrease inferior to 0.1 μM. Taking into account that the matrix volume is about three orders of magnitude lower than the outside one, we set the buffer capacity to B = 300 000.

The numeric solution of the system of differential equations was performed using the software 'Pspice', aimed at solving rigid systems of differential equation, or with a home-made software using the method of backward integration with variable steps. The two methods provided identical solutions.

3. Results and discussion

The model described above, and schematically represented in Fig. 1, takes into account two main experimental results: (i) PTP opening and closure are induced by changes in pH_i [15]; and (ii) PTP opening induces an inhibition of the respiration rate [12]. We show here that these two important features are sufficient to account for the various mCICR profiles, i.e. for the generation of Ca^{2+} oscillations and spikes by mitochondria. Our model does not take into account the $2Na^+/Ca^{2+}$ or $Ca^{2+}/2H^+$ exchangers which are not operative in our experimental generation of calcium spikes [9,10]. Although calcium oscillations are rarely observed in mitochondria and not in the conditions in which we observe calcium spiking, our aim in simulating calcium oscillations is to show what parameters have to be varied in order to obtain an excitable organelle exhibiting calcium spiking behaviour.

The simulation of the mitochondrial response to Ca^{2+} stimulation corresponding to the parameter values given above, is presented in Fig. 2. After Ca^{2+} addition, Ca^{2+} is taken up by mitochondria according to Eq. (2), and induces the following processes: the electrogenic uptake of Ca^{2+} decreases $\Delta\Psi$, this decrease causes an increase of the respiration rate, according to Eq. (7) and Eq. (8), and thus, a H^+ efflux leading to matrix alcalinization. Such increase in pH_i

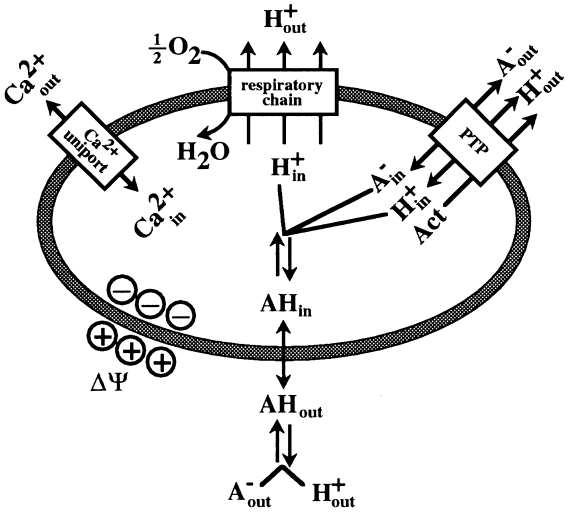

Fig. 1. Schematic representation of the model components. See model description in the text.

triggers PTP opening according to the function *f* and Eq. (3) and Eq. (4). Prior to PTP opening, the activation of respiration leads to a slight transient increase of $\Delta\Psi$, but then, PTP opens and anion and H^+ fluxes proceed (Eq. (5) and Eq. (6)), resulting in a decrease of $\Delta\Psi$, and thus, in the efflux of Ca^{2+} through the uniporter. Ca^{2+} efflux proceeds until the equilibrium state between internal exchangeable Ca^{2+} and external Ca^{2+} concentration is reached. Simultaneously, pH_i partially recovers due to the decrease of respiration rate caused by the efflux of activator, and to the influx of H^+ through the PTP. However, in this simulation, pH_i recovery is not sufficient to close the PTP. Fig. 2 thus simulates the PTP sustained opening mode [15].

Ca^{2+} oscillations and spikes due to mCICR depend on a PTP transitory opening mode [9,12,13], that our model does not simulate with the parameter values used in Fig. 2. Under the conditions of Fig. 2, a very weak efflux of respiration activator proceeds during PTP opening, thus a high respiration rate and a high H^+ efflux are maintained during PTP opening, that sustain a high pH_i. This is the reason why the PTP remains permanently open. Paradoxically, the only way to obtain a re-uptake of Ca^{2+} is to slow down the respiratory rate to decrease pH_i.

This can be achieved by increasing the efflux of the respiration activator through the PTP during channel opening. (Fig. 3). As a result of the faster activator loss during PTP opening, respiration remains inhibited for a longer time, which allows a significant decrease of pH_i, and thus, the partial closure of the PTP. PTP closure then stops the activator efflux, and then, according to our hypothesis of continuous activator supply, the respiratory rate starts increasing again, as well as pH_i, which results in PTP re-opening. Then the cycle (Fig. 4) repeats, and leads to Ca^{2+} oscillations. Ca^{2+} initiates the oscillatory process by acceleration of respiration and by converting the electric part of $\Delta\Psi$ into an increase in pH_i that leads to PTP opening. This is the way by which the activation status of the PTP is connected with the respiratory rate. The transition from monotonous kinetics of Ca^{2+} efflux (Fig. 2) to damped oscillations (Fig. 3) as observed in [12] is obtained by increasing the respiration inhibition during PTP opening, thus decreasing pH_i to values that allow the partial closure

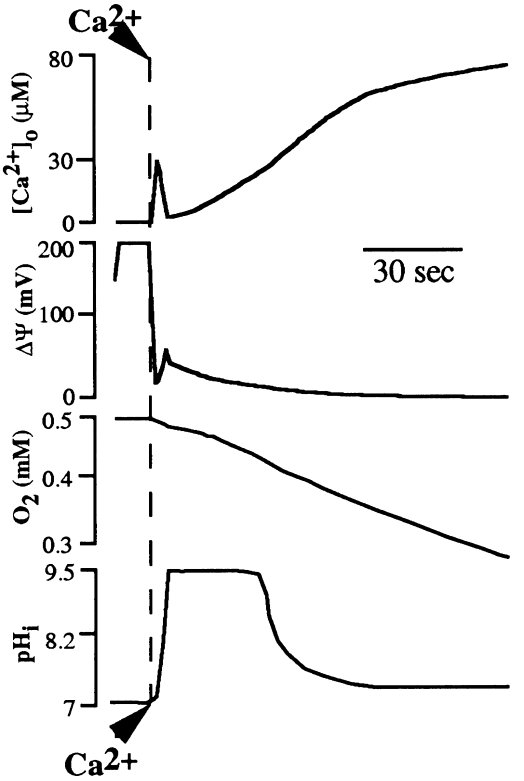

Fig. 2. Simulation of sustained mCICR in response to an external Ca^{2+} pulse. Extramitochondrial Ca^{2+} concentration at the moment of stimulation: 30 μM. All parameter values are presented in the text (model description). Kinetics of extramitochondrial Ca^{2+} concentration ($[Ca^{2+}]_0$), $\Delta\Psi$, extramitochondrial oxygen (O_2), and pH_i. Concentration in protein is set equal to 2 mg ml^{-1}.

of the PTP. The damping can be decreased by globally increasing the membrane and channel permeabilities, leading to sustained oscillations (Figs. 5 and 6) as experimentally observed in [13].

We will now consider the mCICR triggering features exhibited by the model. Fig. 6 shows a simulation of the mitochondrial response to Ca^{2+} stimulation pulses of various amplitudes, using the same settings as in Fig. 5. If the amount of added Ca^{2+} is sufficient for inducing PTP opening (Fig. 6A), the mitochondrial response varies only slightly when the amount of Ca^{2+} used as stimulus is further increased. For instance, the trace shown in Fig. 5 was obtained using twice more Ca^{2+} as stimulus than in Fig. 6A (respectively, 30 and 16 μM Ca^{2+}). On the contrary, a very slight decrease of the stimulus under a threshold value (15.5 μM Ca^{2+} in Fig. 6B, instead of 16 μM Ca^{2+} in Fig. 6A), results in quite different response

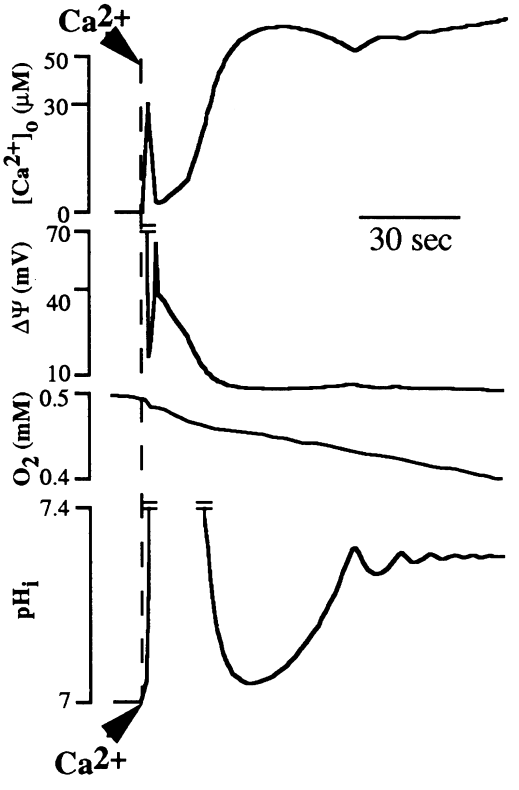

Fig. 3. Simulation of a damped mCICR oscillatory regime, obtained by increasing the efflux of respiration activator during PTP opening. Variables and parameter values are as in Fig. 2, except P_A = 20 min^{-1}.

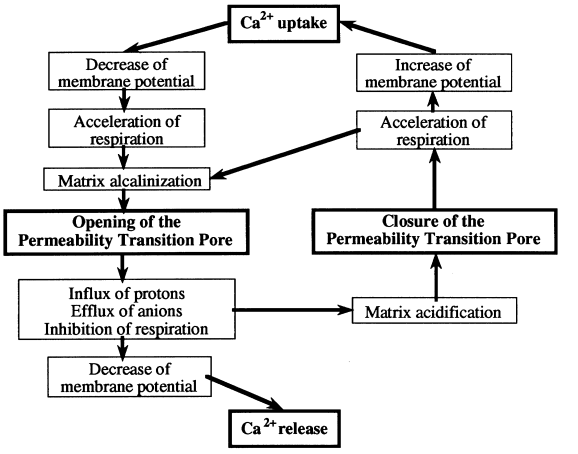

Fig. 4. Sequence of events leading to mCICR.

(Fig. 6B). In the latter case, the stimulus does not trigger PTP opening, and the Ca^{2+} provided is simply buffered by mitochondrial Ca^{2+} uptake. The model thus simulates the two main features of mCICR, i.e. the threshold-dependence of mCICR triggering, and the all-or-nothing nature of the mCICR response [9].

Fig. 7 shows that the model can also simulate the dependence of mCICR triggering on the frequency of Ca^{2+} stimulation pulses (see Fig. e,f in Ref. [9]).

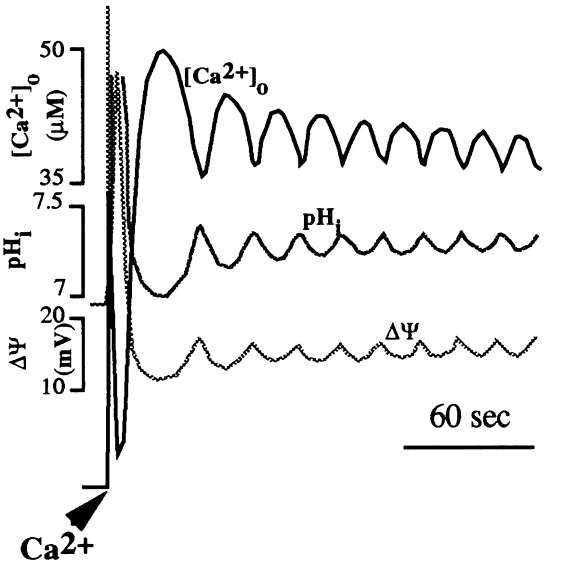

Fig. 5. Simulation of a sustained mCICR oscillatory regime. Parameter values are as in Fig. 3, except P_A = 500 min^{-1}, P_H = 500 min^{-1} mV^{-1} mg protein^{-1}, P_{An}=0.006 min^{-1} mV^{-1} mg protein^{-1}, k_{AH} = 300 min^{-1} mg protein^{-1}, k_F^{op}8 min^{-1}.

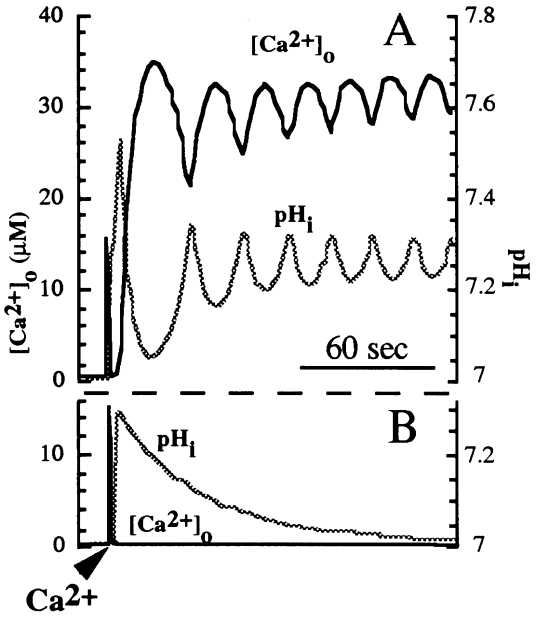

Fig. 6. Simulation of $[Ca^{2+}]_0$, and pH_i kinetics in response to different amplitudes of Ca^{2+} stimulation. Parameter values are as in Fig. 5. (A) Ca^{2+} stimulation 16 μM, (B) Ca^{2+} stimulation 15.5 μM.

Experimentally, in response to a fixed cumulated amount of Ca^{2+} delivered as a series of pulses, mitochondria undergo mCICR depending on the frequency of the stimulation pulses. This means that the triggering threshold of mCICR is not a constant in terms of Ca^{2+} amount, but depends on the rate at which Ca^{2+} is provided to mitochondria [9]. Fig. 7 shows a simulation of this feature. Three stimulations with a period of 0.5 min do not induce PTP opening (Fig. 7B), while the same stimulations performed with a period of 0.2 min induce PTP opening (Fig. 7A), and further Ca^{2+} oscillations. The amount of Ca^{2+} taken up by mitochondria at the end of the stimulation sequence is the same in both cases, as well as the value of $\Delta\Psi$. In both cases, the amplitude of the $\Delta\Psi$ drops, that respond to the stimulation pulses, is constant. A very similar situation is observed experimentally [9]. On the other hand, the recovery of pH_i is a much slower process than recovery of $\Delta\Psi$ or than the uptake of added Ca^{2+}. Therefore, the higher the frequency of stimulation, the higher the initial pH_i value at the time of each stimulation pulse. Thus, among the factors triggering PTP opening, pH_i is sufficient to account for the rate-dependence of mCICR triggering. Our recent experimental observations [10], and the present model analysis, show that pH_i is the key factor regulating the PTP activation status during mCICR.

As shown in Fig. 6, the probability of PTP opening sharply depends on the initial Ca^{2+} amount used as stimulus, because the latter is connected stoicheometrically with H^+ respiratory efflux. However, the maximal pH_i level reached during Ca^{2+} uptake depends

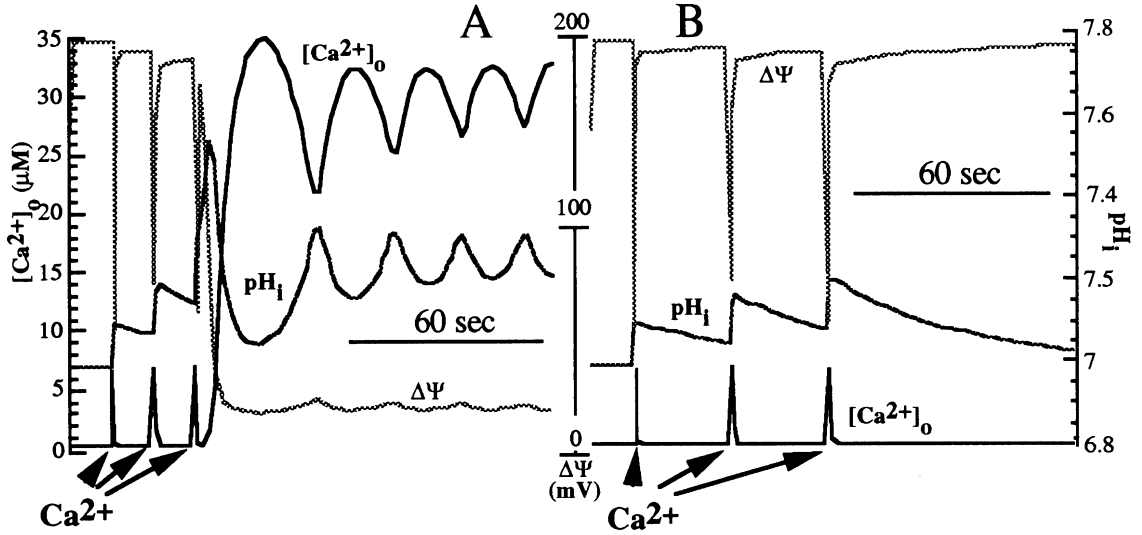

Fig. 7. Simulation of $[Ca^{2+}]_0$, $\Delta\Psi$, and pH_i kinetics in response to series of under-threshold Ca^{2+} pulses of variable frequencies. Value of each Ca^{2+} pulse is 7 μM. (A) Time interval between pulses 0.2 min. (B) Time interval between pulses 0.5 min; other parameters as in Fig. 5.

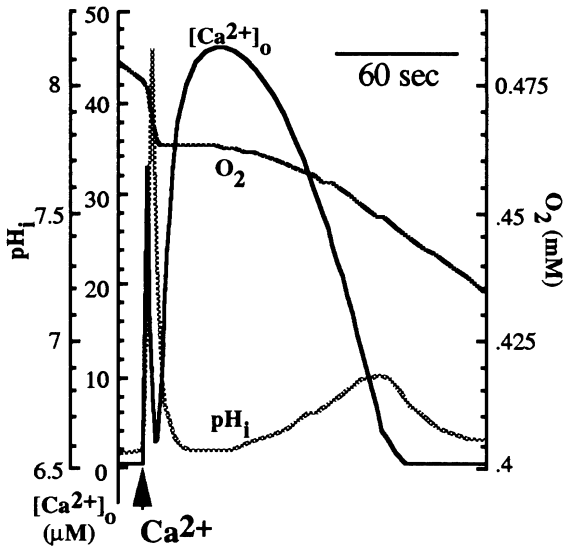

Fig. 8. Simulation of a mCICR spike, obtained by increasing the electroneutral flux of weak acids; k_{AH} = 300 min^{-1} mg $protein^{-1}$. Other parameters as in Fig. 6A.

also on the opposite electroneutral flux of weak acids (Eq. (13)) which buffers the pH_i changes. This effect is particularly apparent in Fig. 7: due to the electroneutral flux of weak acids, pH_i recovers when the time interval between stimulations is long, thus, mitochondria can take up more Ca^{2+} without activation of the PTP. The decrease of the respiration rate that occurs after PTP opening also contributes to pH_i recovery. Indeed, the slower the respiration rate, and hence the smaller its ratio to the electroneutral flux, the more Ca^{2+} taken-up before pH_i reaches the value triggering PTP opening. At slower respiratory H^+ efflux and faster opposite electroneutral flux, the equilibrium between this two fluxes can be reached at low pH_i values that do not trigger PTP opening. One can suppose that in these conditions, all the Ca^{2+} released could then be taken-up without re-activation of the PTP. Fig. 8 presents such a simulation, where the respiration rate is low and the electroneutral flux of weak acids high. In these conditions, a single Ca^{2+} spike is simulated. Immediately after Ca^{2+} stimulation, the respiration rate strongly increases, resulting in a consequent increase of pH_i. Then, after Ca^{2+} release, only a slight increase of the respiration rate and of pH_i takes place, although all released Ca^{2+} is taken up again. Such single spikes represent an important mode of mCICR [9].

Further improvements of the model are currently studied in our laboratory: they concern (i) the modelling of the calcium fluxes through the calcium uniporter; recently Magnus and Keizer [27] introduced an allosteric term in the calcium flux equation in order to account for data of Wingrove et al. [20]. This is certainly a better model to account for the threshold observed in the calcium concentration for calcium influx.

(ii) Another important point concerns the modelling of the calcium pools inside mitochondria; a 100 μM free internal calcium is certainly unrealistic, but however the amount of calcium uptake by mitochondria is huge under bound form; thus a bound calcium pool has to be considered that becomes releasable after a $\Delta\Psi$ collapse.

The model presented here however, simulates all the mCICR profiles observed experimentally, as well as the notable triggering characteristics of mCICR. Since mCICR contributes to cell Ca^{2+} signalling [9,10], the model we present here should appear useful to further mathematically address the role of mCICR in the spatiotemporal organisation of intracellular Ca^{2+} signals as already proposed by Meyer and Stryer [28].

Acknowledgements

We are deeply indebted to Dr. R. Thomas for his help, and to Drs. P. Bernardi, A. Goldbeter, J.B. Hoek, J. Keizer and D.G. Nicholls for scientific advice and critical reading of the manuscript. This work was funded by la Ligue Contre le Cancer (L.C.C.), l'AFM, la Région Aquitaine, and la FRM. L.S.J. was supported by la L.C.C.

References

[1] S. Miyazaki, Curr. Opin. Cell Biol. 7 (1995) 190.
[2] X. Gu, N.C. Spitzer, Nature 375 (1995) 784.
[3] M.J. Berridge, Nature 361 (1993) 315.
[4] J.D. Lechleiter, D.E. Clapham, Cell 69 (1992) 283.
[5] R. Rizzuto, M. Brini, M. Murgia, T. Pozzan, Science 262 (1993) 744.
[6] L.S. Jouaville, F. Ichas, E.L. Holmuhamedov, P. Camacho, J.D. Lechleiter, Nature 377 (1995) 438.
[7] S.L. Budd, D.G. Nicholls, J. Neurochem. 66 (1996) 403.

[] P.B. Simpson, J.T. Russel, J. Biol. Chem. 271 (1996) 33493.
[9] F. Ichas, L.S. Jouaville, S.S. Sidash, J.-P. Mazat, E.L. Holmuhamedov, FEBS Lett. 348 (1994) 211.
[10] F. Ichas, L.S. Jouaville, J.-P. Mazat, Cell 89 (1997) 1145.
[11] D.D. Friel, R.W. Tsien, J. Neurosci. 14 (1994) 4007.
[12] Y.U. Evtodienko, V.V. Teplova, J. Khawaja, N.E.L. Saris, Cell Calcium 15 (1994) 143.
[13] Y.V. Kim, L.Y. Kudzina, V.P. Zinchenko, Y.V. Evtodienko, Eur. J. Biochem. 153 (1985) 503.
[14] T.E. Gunter, K.K. Gunter, S.S. Sheu, C.E. Gavin, Am. J. Physiol. 267 (1994) C313.
[15] M. Zoratti, I. Szabò, Biochim. Biophys. Acta 1241 (1995) 139.
[16] A. Atri, J. Amundson, D. Clapham, J. Sneyd, Biophys. J. 65 (1993) 1727.
[17] G. Dupont, A. Goldbeter, BioEssays 14 (1992) 485.
[18] G. Dupont, A. Goldbeter, Cell Calcium 14 (1993) 311.
[19] G. De Young, J. Keizer, Proc. Natl. Acad. Sci. USA 89 (1992) 9895.
[20] D.E. Wingrove, J.M. Amartruda, T.E. Gunter, J. Biol. Chem. 259 (1984) 9390.
[21] K.E. Coll, S.K. Joseph, B.E. Corkey, J.R. Williamson, J. Biol. Chem. 257 (1982) 8696.
[22] F. Ichas, PhD Thesis, Bordeaux, France, 1997.
[23] G.M. Heaton, D.G. Nicholls, Biochem. J. 156 (1976) 635.
[24] R.B. Gennis, Biomembranes: Molecular Structure and Functions, NewYork, 1989.
[25] S. Massari, L. Frigeri, G. Azzone, J. Membrane Biol. 9 (1972) 57.
[26] C.P. Connern, A.P. Halestrap, Biochemistry 35 (1996) 8172.
[27] G. Magnus, J. Keizer, Am. J. Physiol. 273 (1997) C717.
[28] T. Meyer, L. Stryer, Proc. Natl. Acad. Sci. USA 85 (1988) 5051.